Revealing the UV response of melanocytes in xeroderma pigmentosum group A using patient-derived induced pluripotent stem cells

Takemori, Chihiro ; Koyanagi-Aoi, Michiyo ; Fukumoto, Takeshi ; Kunisada, Makoto ; Wakamatsu, Kazumasa ; Ito, Shosuke ; Hosaka, Chieko…

(Citation)
Journal of Dermatological Science,115(3):111-120

(Issue Date)
2024-09-17

(Resource Type)
journal article

(Version)
Version of Record

(URL)
https://hdl.handle.net/20.500.14094/0100495953

Journal of Dermatological Science 115 (2024) 111–120

Contents lists available at ScienceDirect

Journal of Dermatological Science

journal homepage: www.elsevier.com/locate/jdermsci

Original Article

Revealing the UV response of melanocytes in xeroderma pigmentosum group A using patient-derived induced pluripotent stem cells

Chihiro Takemori [a,1], Michiyo Koyanagi-Aoi [b,c,d,1], Takeshi Fukumoto [a,1], Makoto Kunisada [a,e], Kazumasa Wakamatsu [f], Shosuke Ito [f], Chieko Hosaka [a], Seiji Takeuchi [a], Akiharu Kubo [a], Takashi Aoi [b,c,d,*], Chikako Nishigori [a,c,**]

[a] Division of Dermatology, Department of Internal Related, Graduate School of Medicine, Kobe University, Kobe, Japan
[b] Division of Stem Cell Medicine, Graduate School of Medicine, Kobe University, Kobe, Japan
[c] Division of Advanced Medical Science, Graduate School of Science, Technology and Innovation, Kobe University, Kobe, Japan
[d] Center for Human Resource development for Regenerative Medicine, Kobe University Hospital, Kobe, Japan
[e] Department of Dermatology, Hyogo Prefectural Harima-Himeji General Medical Center, Himeji, Japan
[f] Institute for Melanin Chemistry, Fujita Health University, Toyoake, Japan

ARTICLE INFO

Article history:
Received 25 October 2023
Received in revised form 16 April 2024
Accepted 14 June 2024

Keywords:
Xeroderma pigmentosum
iPS cells
Melanocytes
Ultraviolet radiation
Microarray
DNA repair

ABSTRACT

Background: Xeroderma pigmentosum (XP) is characterized by photosensitivity that causes pigmentary disorder and predisposition to skin cancers on sunlight-exposed areas due to DNA repair deficiency. Patients with XP group A (XP-A) develop freckle-like pigmented maculae and depigmented maculae within a year unless strict sun-protection is enforced. Although it is crucial to study pigment cells (melanocytes: MCs) as disease target cells, establishing MCs in primary cultures is challenging.
Objective: Elucidation of the disease pathogenesis by comparison between MCs differentiated from XP-A induced pluripotent stem cells (iPSCs) and healthy control iPSCs on the response to UV irradiation.
Methods: iPSCs were established from a XP-A fibroblasts and differentiated into MCs. Differences in gene expression profiles between XP-A-iPSC-derived melanocytes (XP-A-iMCs) and Healthy control iPSC-derived MCs (HC-iMCs) were analyzed 4 and 12 h after irradiation with 30 or 150 J/m^2 of UV-B using microarray analysis.
Results: XP-A-iMCs expressed SOX10, MITF, and TYR, and showed melanin synthesis. Further, XP-A-iMCs showed reduced DNA repair ability. Gene expression profile between XP-A-iMCs and HC-iMCs revealed that, numerous gene probes that were specifically upregulated or downregulated in XP-A-iMCs after 150-J/m^2 of UV-B irradiation did not return to basal levels. Of note that apoptotic pathways were highly upregulated at 150 J/m^2 UV exposure in XP-A-iMCs, and cytokine-related pathways were upregulated even at 30 J/m^2 UV exposure.
Conclusion: We revealed for the first time that cytokine-related pathways were upregulated even at low-dose UV exposure in XP-A-iMCs. Disease-specific iPSCs are useful to elucidate the disease pathogenesis and develop treatment strategies of XP.

1. Introduction

Xeroderma pigmentosum (XP) is an autosomal recessive disorder characterized by photosensitivity, including accelerated photoaging characteristics; freckle-like pigmented maculae and depigmented maculae and predisposition to skin cancers in sunlight-exposed areas from younger ages. XP is classified into eight molecular and clinical subtypes; groups A–G, which are deficient in nucleotide excision repair (NER) [1], and XP variant, that is deficient in translesion DNA synthesis but proficient with NER. NER is responsible for the repair/removal of UV-induced DNA photolesions, including

* Corresponding author at: Division of Stem Cell Medicine Graduate School of Medicine, Kobe University, 7-5-1 Kusunoki-cho, Chuo-ku, Kobe 650-0017, Japan.
** Corresponding author at: Division of Dermatology, Department of Internal Related, Kobe University Graduate School of Medicine, 7-5-1 Kusunoki-cho, Chuo-ku, Kobe 650-0017, Japan.
E-mail addresses: takaaoi@med.kobe-u.ac.jp (T. Aoi), chikako@med.kobe-u.ac.jp (C. Nishigori).
[1] These authors contributed equally to this study.

https://doi.org/10.1016/j.jdermsci.2024.06.004

cyclobutane pyrimidine dimers and pyrimidine pyrimidone (6–4) pyrimidone photoproducts ((6–4)PP). NER deficiency causes the accumulation of DNA photolesions, which induce genomic mutations, causing the failure to produce proper proteins, leading to cellular death or dysfunction and may cause skin cancers that can manifest as clinical symptoms [1,2]. NER consists of two pathways; Transcription-Coupled NER(TC-NER) pathways and Global Genome NER (GG-NER) pathways. XP-A, XP-B, XP-D, XP-F and XP-G are deficient in TC-NER pathways and they manifest exaggerated sunburn upon minimum sun exposure and varied degree of neurological symptoms.

XP-A constitutes approximately 50 % of Japanese XP population and 90 % of them harbor homozygous mutation of g.15148 G > C (c.390–1 G > C), which is a founder mutation of Japanese XP-A [3,4], that creates aberrant splicing, resulting in premature termination. Patients with XP-A present with the lowest NER ability and severe cutaneous and neurological symptoms: they typically develop severe sunburn upon initial exposure to sunlight after birth, which subsides after 10–14 days, followed by formations of freckle-like pigmented and/or depigmented maculae, which gradually increase in number [2]. These pigmentary changes usually occur before 1 year of age and can develop into cutaneous cancers around 7–9 years of age unless strict photoprotection is enforced, while the earliest signs of neurologic symptoms, such as sensorineural hearing impairment and stumbling appear after 6 years of age.

Pathogenesis in XP is poorly understood. To clarify the pathogenesis of XP, it is crucial to study symptomatic status of target organs and cells, such as cutaneous and neurologic representations. Among them, pigmentary symptoms are inevitable and observed within 12 months. Hence, in this study, melanocytes (MCs) were selected as target cells to investigate the pathogenesis of XP-A, the severest type of XP.

To obtain XP-A patients derived MCs, induced pluripotent stem cells (iPSCs) were generated [5]. This technology has enabled the generation of patient-derived iPSCs to recapitulate pathological conditions and drug discovery. Although there have been some reports on XP-A-iPSCs [6,7], differentiation of XP-A-iPSCs into MCs has never been reported. Few studies have examined how accumulation of DNA photolesions in MC affect XP-A symptoms, because of the challenge of establishing primary culture of MCs [8].

We generated MC precursor cells (MPCs) from iPSCs in 2019 [8]. MPCs are self-renewable and can differentiate into MCs in 1 week after inhibiting glycogen synthase kinase 3 beta. The use of MPCs makes it feasible to obtain MCs. Here, MCs were established from XP-A patient derived iPSCs to investigate the molecular mechanisms underlying the development of abnormal pigmentary symptoms associated with XP-A.

2. Materials and methods

2.1. Establishment of human iPSC lines from fibroblasts

Human diploid fibroblasts from healthy control skin (TIG-120 cells; JCRB0542) and fibroblasts derived from a patient with XP-A (XP3OS) are used for establishments of human iPSC lineste. XP3OS cells (JCRB0303) are known to have the Japanese founder mutation of *XPA* (c.390–1 G > C: g. 15148 G > C) [3]. hiPSC lines were established from these two fibroblast strains using the CytoTune-iPS 2.0 Sendai Reprogramming Kit (ID Pharma Co., Ltd., Tsukuba, Japan) as previously described [8].

2.2. Differentiation of feeder-free iPSCs into MPCs and melanocytes

Feeder-free iPSCs were differentiated into MPCs and MCs as previously described [8]. MPCs could be subjected to repeated passage in fibronectin-coated dishes with TrypLE™ Select recombinant enzyme (Thermo Fisher). MPCs cultured in Medium 254 with HMGS were differentiated into MCs approximately 1 week after adding 3 μM CHIR99021 every 2 days. Alternatively, melanocytes which were not obtained through differentiation of MPCs were available by changing the complex medium to Medium 254 containing HMGS and 3 μM CHIR99021.

2.3. Flow cytometry-based NER assay

Removal of DNA photolesion was assessed using flow cytometry as previously described [9]. We used UV-C for the repair assay, because DNA photolesion, which XP cells fail to repair, are most efficiently produced around 260 nm UV [10]. In fact, DNA repair assay for XP have usually performed using UV-C germicidal lamps, at clinical setting for diagnosis as well as research [9]. Briefly, the cells were irradiated with 30 J/m^2 UV-C, and harvested immediately or 6 h after irradiation. Subsequently, the cells were stained with a primary monoclonal antibody against (6–4) PP (Cosmo Bio Co., Ltd., Tokyo, Japan) for 1.5 h at 22°C, followed by resuspended in PBS-TB containing Alexa Fluor 488 antibody (Thermo Fisher Scientific) for 1 h at 22°C, and then, resuspended in PBS containing 5 μg/ml propidium iodide (Thermo Fisher). The rate of DNA photolesion removal was calculated based on the average fluorescence intensity. The fluorescence intensity of cells without UV irradiation was considered background and that of cells immediately after UV irradiation as 100 %. The reduction in fluorescence intensity was measured at 6 h.

2.4. Quantification of melanin in iPSCs derived melanocytes and effect of UV-B irradiation on melanin synthesis

Melanin content in iPSCs-derived melanocytes and NHEMs were quantified before and 24 h after UV-B irradiation using HPLC as previously described [11–13]. We used UV-B because patients with XP-A develop cutaneous symptoms after sun exposure and sunlight reaches to the surface of the earth includes UV-B and UV-A, but not UV-C. UVB has biologically stronger impact than UV-A and most clinically prominent symptoms are caused by UV-B. Therefore, we used UV-B for the study in view of giving us insights on XP clinical symptoms including melanin quantification. In order to obtain the optimum UV-B dose to investigate the melanocytes biology in XP, we used viability assay using UV-B (S-text).

2.5. Microarray data

The microarray data of normal human epidermal MCs (NHEMs), healthy control iPSC-derived MCs (HC-iMCs), and XP-A-iPSC-derived MCs (XP-A-iMCs) were deposited into the Gene Expression Omnibus (GEO) database under accession number GSE185308. Raw data of the basal expression level for XP-A and HC-control fibroblasts are available at GEO (http://www.ncbi.nlm.nih.gov/geo/) under accession number GSE70818 [14].

3. Results

3.1. Generation of iPSCs from XP-A patient-derived fibroblasts

To generate XP-A-iPSCs and HC-iPSCs, SeV vectors coding OCT3/4, SOX2, C-MYC, and KLF4 were transduced into XP3OS and TIG120. Cell morphologies of TIG120 (HC) and XP3OS (XP-A) are shown in Fig. 1A left panels. Colonies were picked up three weeks after transduction, the expanded clones 21F2 (HC) and 38B3 (XP-A) displayed typical hESC-like morphologies (Fig. 1A right panels). Semi-quantitative RT-PCR indicated that these clones expressed OCT3/4, SOX2, and NANOG at the mRNA level and did not harbor the SeV vector (Fig. 1B). Immunofluorescence staining confirmed the expression of the pluripotent markers OCT3/4, SOX2, and NANOG at the protein level (Fig. 1C, Fig.

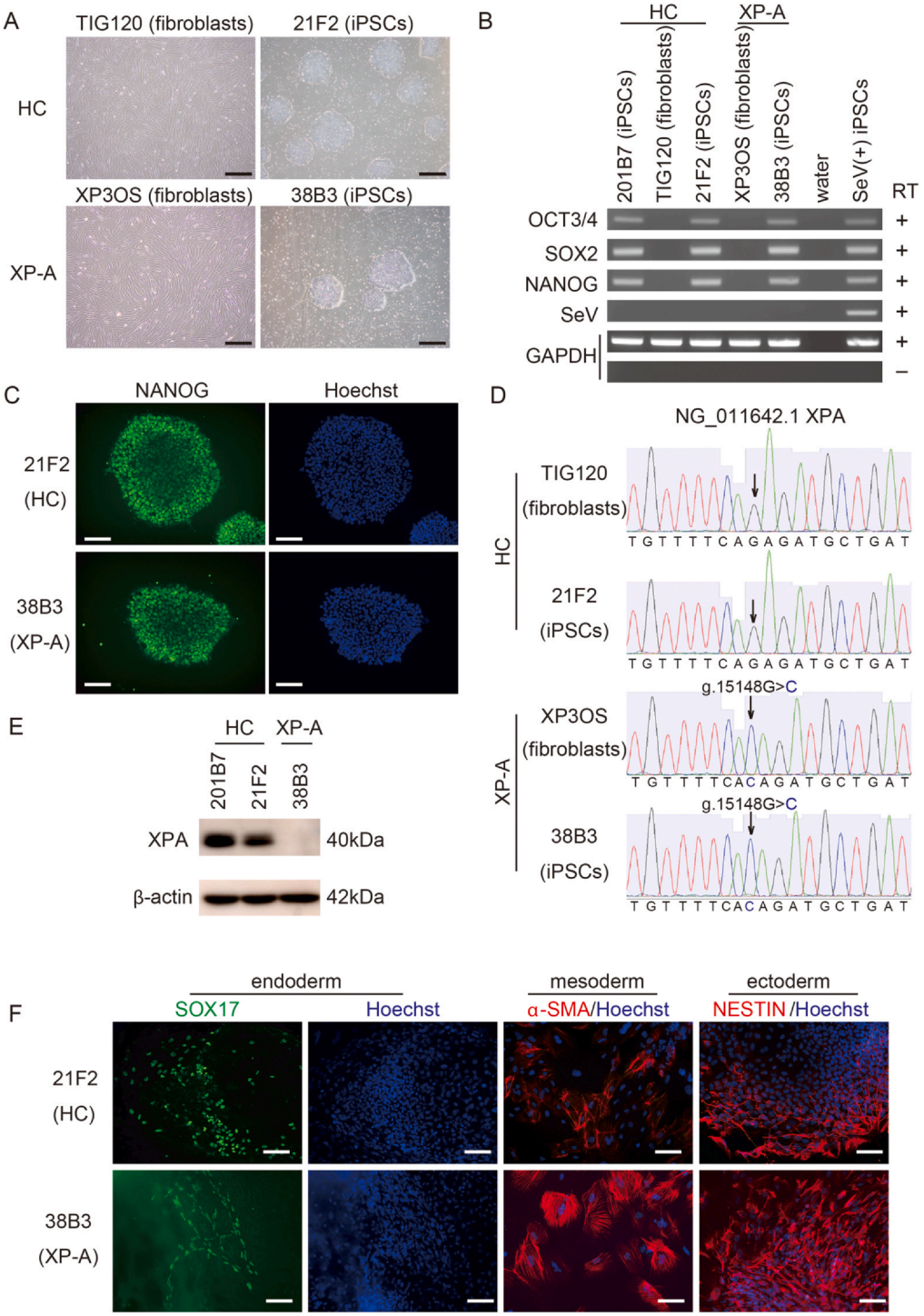

Fig. 1. The generation of iPSCs from an XP-A patient and a healthy control (HC).
(A) Morphologies of HC fibroblasts (TIG120, left upper panel) and XP-A patient-derived fibroblasts (XP3OS, left lower panel). Picked-up clones 21F2 and 38B3 showed hESC-like morphologies (upper and lower panels in the right, respectively). Scale bar = 500 μm (B) Semi-quantitative RT-PCR analyses of pluripotent marker genes (OCT3/4, SOX2, and NANOG) and SeV in fibroblasts, established clones 21F2 and 38B3, and conventional iPSC clone 201B7. GAPDH was used as a loading control. RT, reverse transcriptase. (C) Immunofluorescence analysis of the expression of the pluripotency marker NANOG. Nuclei were stained with Hoechst 33342. Scale bar = 100 μm (D) Genomic sequencing validated the *XPA* mutation g.15148 G > C in the 38B3 clone.(E) Immunoblotting analysis of *XPA* in human iPSC clones. β-actin was used as a loading control.(F) Immunostaining of *in vitro* EB-mediated differentiated cells stained for markers specific of all three germ layers: SOX17 (endoderm, left two panels), α-SMA (mesoderm, middle panels), and NESTIN (ectoderm, right panels). Nuclei were stained with Hoechst 33342. Scale bar = 100 μm.

S1A). Both clones had a 46XX normal karyotype (Fig. S1B). Gene sequencing of 38B3 revealed the same mutation in *XPA* as that in corresponding fibroblasts, XP3OS (Fig. 1D). 38B3 did not express the XPA protein (Fig. 1E). *In vitro* differentiation through EB formation confirmed the ability of both clones to differentiate into cells of the three germ layers spontaneously, including SOX17-positive endoderm, α-SMA-positive mesoderm, and NESTIN-positive ectoderm (Fig. 1F), indicating that HC and XP-A fibroblasts were successfully reprogrammed into a pluripotent state. The clones 21F2 and 38B3 were used for further evaluation.

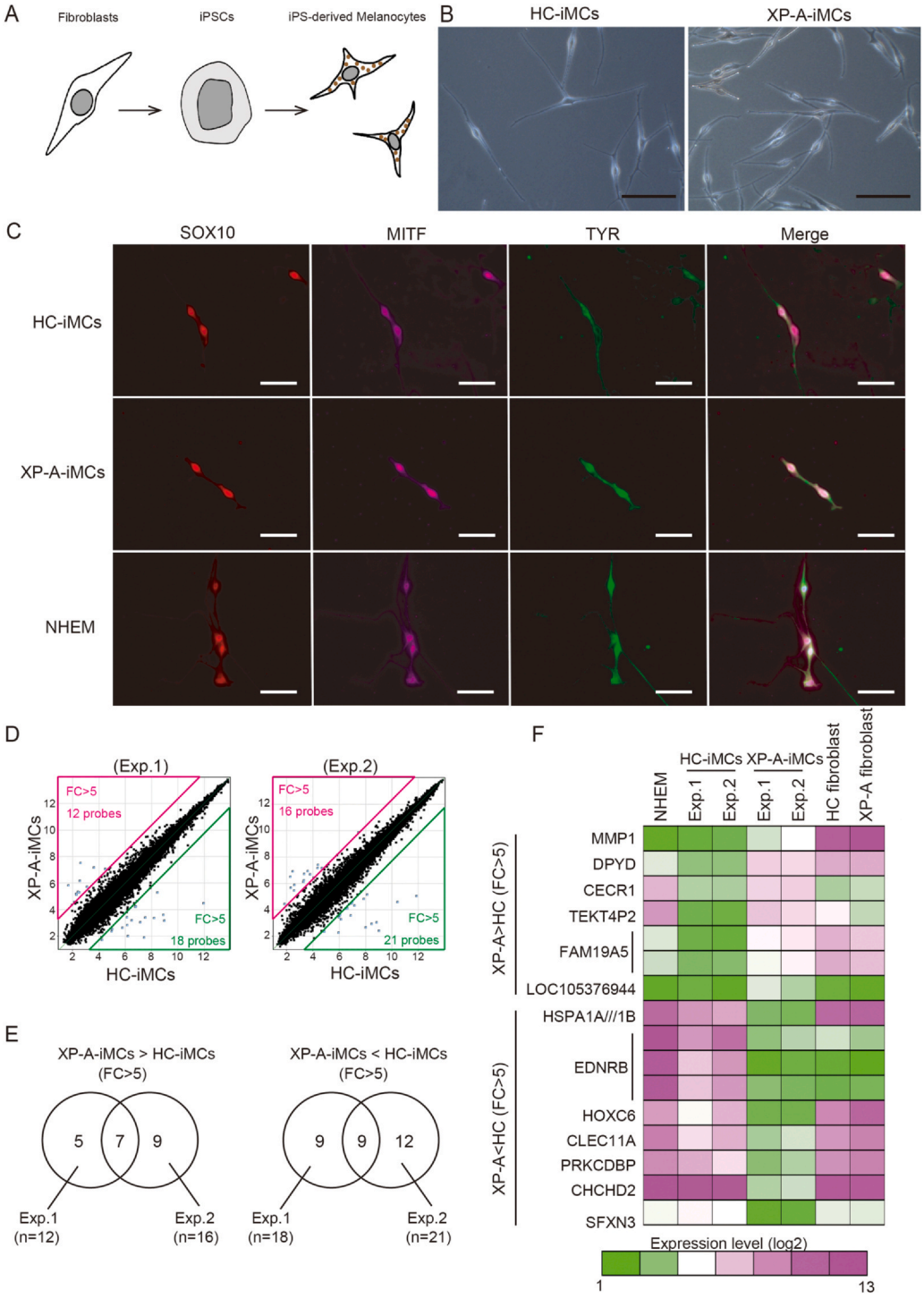

Fig. 2. The generation of MCs from healthy control and XP-A iPSCs.
(A) Differentiation from HC and XP-A iPSCs to MCs. (B) Cell morphology of HC- and XP-A iPSC-derived MCs under a phase-contrast microscope. Scale bar = 100 μm (C) Immunofluorescence staining of HC- and XP-A iPSC-derived MCs positive for MC markers SOX10, MITF, and TYR. NHEM was used as a positive control. Merged images of SOX10, MITF, TYR, and DAPI are shown in right panels. Scale bar = 50 μm (D) Comparison of global gene expression levels between HC-iMCs (*x*-axis) and XP-A-iMCs (*y*-axis) in two experiments (Exp. 1 and 2) by scatterplots. Expression levels are presented as log 2 values. Lines show five-fold variations in gene expression levels. (E) Venn diagram analysis identified differentially expressed probes between HC-iMCs and XP-A-iMCs. The left and right circles represent Exp. 1 and Exp. 2, respectively. The intersection of the two circles represents overlapping differentially expressed probes of the two experiments. (F) Heatmap of 16 differentially expressed probes (seven upregulated and nine downregulated in XP-A-iMCs than in HC-iMCs) in NHEM, HC-iMCs (Exp. 1 and 2), XP-A-iMCs (Exp. 1 and 2), HC fibroblasts, and XP-A fibroblasts.

3.2. Generation of MCs from XP-A patient-derived iPSCs

XP-A-iMCs and HC-iMCs were generated from XP-A-iPSCs (38B3) and HC-iPSCs(21F2), respectively, following a previously reported differentiation protocol [8] (Fig. 2A). XP-A-iPSC- and HC-iPSC-derived differentiated cells were thin and had elongated spindle shaped morphology with dendrites, like cultured NHEMs (Fig. 2B, C). They immunohistochemically expressed MC markers SOX10, MITF, and TYR (Fig. 2C). XPA was expressed in HC-iMCs but not XP-A-iMCs (Fig. S2). To infer the pathophysiology of XP-A, the global gene

expression profiles of XP-A-iMCs and HC-iMCs were compared twice (Experiment 1 and 2). Scatter plots identified 30 probes (12 upregulated and 18 downregulated in XP-A-iMCs) and 37 probes (16 upregulated and 21 downregulated in XP-A-iMCs) as differentially expressed (fold change > 5) in Experiments 1 and 2, respectively (Fig. 2D). Sixteen probes (seven upregulated and nine downregulated in XP-A-iMCs) were selected as differentially expressed probes common to both experiments (Fig. 2E). A heatmap revealed clear differences in the expressions of these 16 probes (13 genes) between XP-A-iMCs and HC-iMCs but not between XP-A and HC fibroblasts [14] (Fig. 2F).

3.3. DNA repair ability and cellular viability of XP-A iMCs upon UV exposure

Flow cytometry-based NER assay after UV-C exposure [9,15,16] were illustrated by histograms of relative signal intensity of (6–4)PP in HC-iMCs and XP-A-iMCs that was un-irradiated, immediately, and 6 h after irradiated with 30 J/m^2 UV-C (Fig. 3A left and right; upper, middle, and lower panels, respectively). Results showed that 96.5 % and 6.1 % of (6–4)PP were repaired within 6 h after UV-C irradiation in HC-iMCs and XP-A-iMCs, respectively. Similar results were obtained from three independent experiments.

Cell viability 24 h after irradiation with 0–20 J/m^2 or 0–200 J/m^2 UV-B was evaluated (Fig. 3B left and right, respectively). The viability of HC-iMCs was similar to that of NHEMs at all doses [17], and was significantly lower than that at baseline at 200 J/m^2, but not at 100 J/m^2, whereas that of XP-A-iMCs was significantly reduced at ≥20 J/m^2 UV-B irradiation (Fig. 3B).

3.4. Quantification of melanin in HC-iMCs and XP-A-iMCs with and without UV irradiation

Content of total melanin were varied among cell strains, but melanin synthesis and composition of melanin were not changed by UV irradiation (Fig. 3C, Fig. S3).

3.5. Changes in gene expressions of HC-iMCs and XP-A-iMCs after UV-B irradiation

Patients with XP-A present with photosensitivity and XP-A cells are hypersensitive to UV. To get insights into clinical manifestation in XP-A, the global gene expression of XP-A-iMCs and HC-iMCs were compared after UV-B irradiation. The gene profiles of XP-A-iMCs and HC-iMCs after UV-B exposure were compared from two aspects: (1) at the same UV doses and (2) at doses with similar biological impacts. Regarding the latter," survival ratio" in the colony formation assay was used, where replication ability (colony formation ability) is considered as "survival." Irradiation of XP-A cells and HC cells with approximately 30 and 150 J/m^2 UV-B, respectively, results in a survival rate of approximately 10 % [18]. Hence, XP-A-iMCs and HC-iMCs were irradiated with UV-B at doses of 30 and 150 J/m^2, respectively, to achieve a survival rate of 10 %. The MTT assay (Fig. 3B) revealed UV-B irradiation at 20–200 J/m^2 rendered the viability > 50 % (Fig. 3B). Irradiation with low-dose (30 J/m^2) or high-dose (150 J/m^2) UV-B was followed by incubation for 4 or 12 h before transcriptional profile analysis (Fig. 4A).

Changes in the gene expressions of *SOX10*, *MITF*, and *TYR* were assessed to determine whether MCs were viable and functional after high-dose UV exposure. The results showed that their expressions were relatively unchanged in both strains 12 h after irradiation even with high-dose UV (Fig. S4).

The number of probes with substantial changes in expression levels (> 10-fold) is shown in Fig. 4B. The number of gene probes upregulated/downregulated 4 h after low dose UV-B irradiation vs pre-irradiation was considerably greater in XP-A-iMCs (72 probes) than HC-iMCs (27 probes). Additionally, the expression levels of several genes did not return to pre-irradiation level even 12 h after irradiation. Nonetheless, the number of genes with significantly changed expression levels was fewer after 12 h of incubation compared with that after 4 h (Fig. 4B, left panel). However, following irradiation with high-dose UV-B, the number of differentially expressed probes substantially increased 12 h after irradiation than that 4 h after irradiation in XP-A-iMCs, whereas decreased after 12 h in HC-iMCs as with low-dose UV-B irradiation.

Next, we picked up 26 or 55 probes, which upregulated or downregulated 10-folds or more 4 h after irradiation with high dose of UV-B in HC-iMCs. The expression levels of these probes 4–12 h after irradiation in HC-iMCs and XP-A-iMCs are shown in Fig. 4C. In HC-iMCs, all probes had returned to their original levels 12 h later, whereas in XP-A-iMCs that of almost all the probes did not return to basal levels, even after 12 h, and remained upregulated/downregulated.

3.6. Functional analysis of specific differentially expressed genes (DEGs) of XP-A-iMCs exposed to UV-B

In NHEMs and HC-iMCs exposed to high-dose UV-B, the expression levels of 11 and 3 probes were upregulated > 10-fold and those of 21 and 42 probes were downregulated > 10-fold, respectively, 12 h after exposure compared with the pre-irradiation levels, whereas in XP-A-iMCs with the same procedure the expression levels of 57 and 147 probes were upregulated and downregulated, respectively (Fig. 5A).

Venn diagram analysis indicated that 49 and 132 probes were specifically upregulated and downregulated, respectively, 12 h after high-dose UV-B irradiation in XP-A-iMCs. The details of these probes are shown in Tables S1 and S2, respectively.

Gene Ontology (GO) analysis ($p < 0.05$) was conducted to elucidate the molecular mechanisms associated with cellular responses to UV-B in XP-A-iMCs. The markers of XP-A-iMCs with expression levels specifically upregulated/downregulated 12 h after high-dose UV-B irradiation are indicated in Tables S3 and S4, respectively. Major GO term category suggested from the 49 specifically upregulated genes in XP-A-iMCs included the terms; regulation of cell death, regulation of cell proliferation, regulation of programmed cell death, regulation of the apoptotic process, and response to external stimuli (Fig. 5D, Table S3), while that from the 132 specifically downregulated genes in XP-iMCs included the terms; cell division, mitotic cell cycle, chromosome segregation, mitotic cell cycle process and cell cycle process (Fig. 5E, Table S4).

Among the 49 probes specifically upregulated in XP-A-iMCs, *ATF3* and *CXCL6* were identified as genes involved in the regulation of cell proliferation and response to external stimuli (Table S1). *ATF3* expression increased in all three MC strains 4 h after UV-B irradiation (Fig. 5F), and it returned to basal levels 12 h after UV-B irradiation in NHEMs and HC-iMCs, while it did not in XP-A-iMCs.

Among the 132 probes specifically downregulated in XP-A-iMCs, genes which are functional in cell cycle regulation, such as *BUB1*, *BUB1B*, *CDC20* and *TOP2A* and *HDAC4* gene which is involved in cell cycle progression and transcriptional regulation were identified (Table S2). HDAC4 expression was decreased in all three MCs 4 h after UV-B irradiation and recovered in NHEMs and HC-iMCs after 12 h, while it tended not to recover in XP-A-iMCs and continued to decrease 12 h after UV irradiation (Fig. 5G).

Lastly, the gene expression profiles of XP-A-iMCs and HC-iMCs were compared after similar biological impacts by UV-B (dose which gives survival rate of 10 %). The expression levels of DEGs of XP-A-iMCs (30 J/m^2) and HC-iMCs (150 J/m^2) were compared 12 h after UV exposure (Fig. S4A Fig. 5A middle panel and Fig. S5A). The specifically upregulated DEGs in XP-A-iMCs 12 h after irradiation with 30 J/m^2 (low-dose) were 11 probes (Fig. S5B). Specifically upregulated

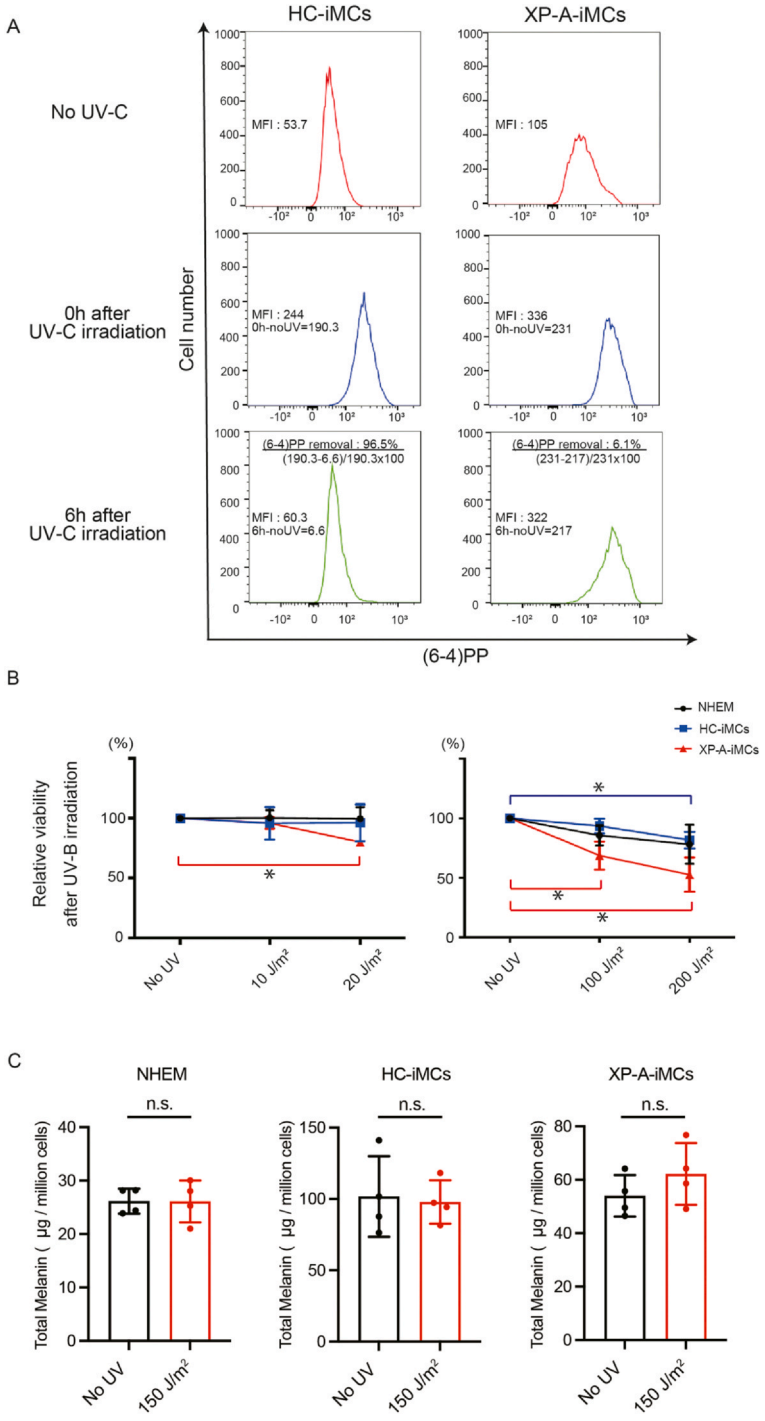

Fig. 3. .Characteristics of MCs from patients with XP-A

(A) Representative histograms illustrating (6–4)PP relative signal intensity, overlaying nonirradiated, immediately after and six hours after irradiation with 30 J/m^2 of UV-C in XP-A-iMCs and HC-iMCs. (B) MTT assay was used to examine cell viability at 24 h after UV-B irradiation. Data from three independent experiments are indicated. Data are presented as the mean ± SD. ANOVA analysis was used for multiple comparisons. *p < 0.05 was considered statistically significant. (C) Content of melanin was chemically determined by HPLC with the combination of alkaline hydrogen peroxide oxidation method and hydrolysis by hydroiodic acid with or without irradiation with 150 J/m^2 of UV-B. Content of eumelanin, benzothiazole-type pheomelanin and benzothiazine-type pheomelanin are represented by PTCA (pyrrole-2,3,5-tricarboxylic acid)×38, TTCA (thiazole-2,4,5-tricarboxylic acid) ×34, and 4-AHP (4-amino-3-hydroxyphenylalanine)×9, respectively as μg/million cells. Total melanin amount was calculated by summing up the above three types of melanin, as previously described [11–13]. Four samples for each point were subjected to the quantification. Data are presented as the mean ± SD. ANOVA analysis was used for multiple comparisons. *p < 0.05 was considered statistically significant.

genes in XP-A MCs after 30 J/m^2 includes *IL11, CXCL6, GREM1* and MMP1 (Table S5). GO analysis indicated that these specifically upregulated genes were associated with 'cytokine activity' and 'cytokine receptor binding (Fig. S5C). A probe for *RBMS3* was specifically downregulated in XP-A-iMCs 12 after UV irradiation with 30 J/m^2 (Table S6), but any specific GO terms were indicated.

4. Discussion

To date, two studies have reported successful establishment of iPSCs from patients with XP and characteristics of XP-iPSCs [6,7]. However, to investigate disease pathophysiology, it is vital to investigate the state of the target organs/cells. In this study, MCs were selected to study the

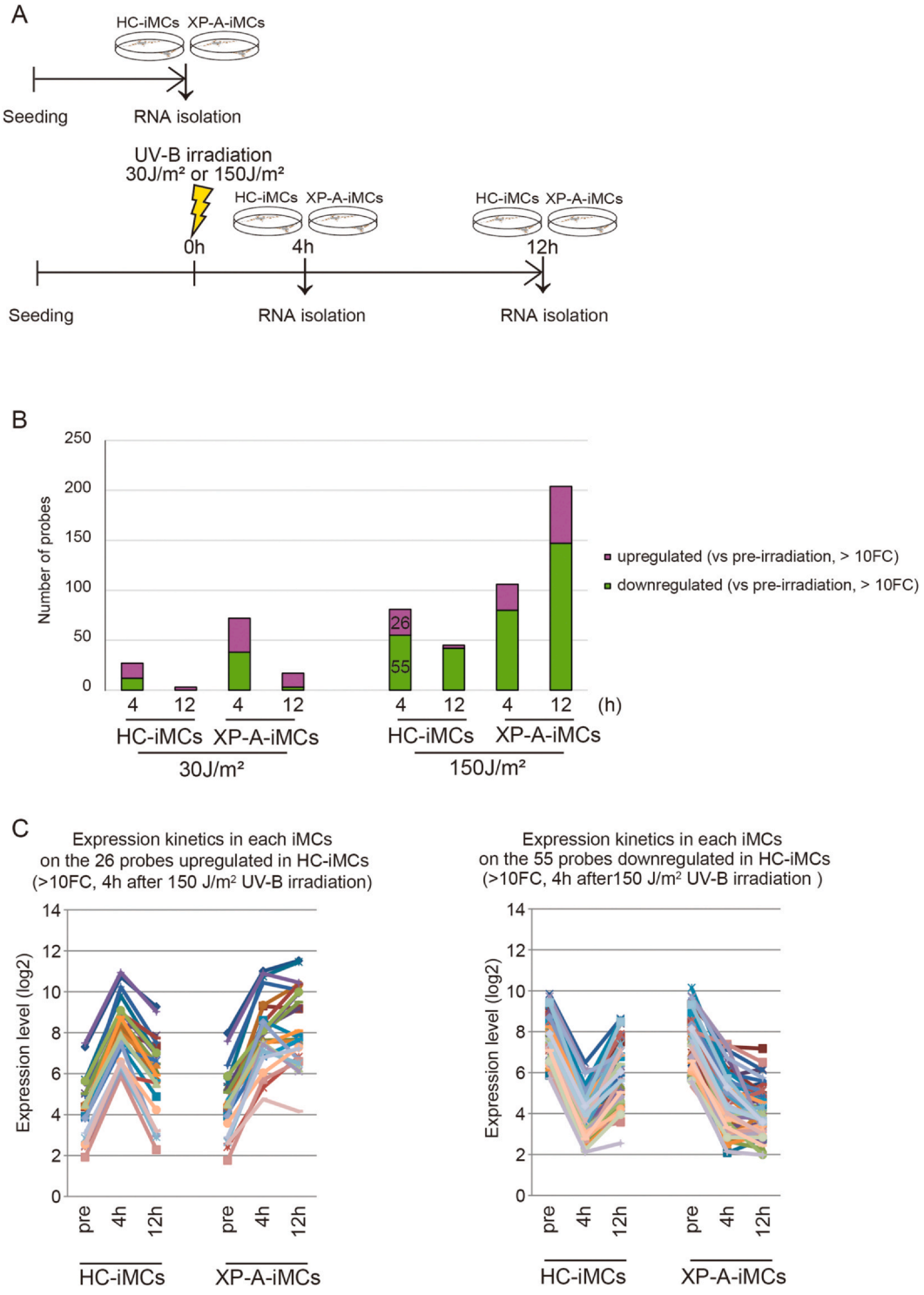

Fig. 4. Comparison of genes affected by UV-B irradiation in HC-iMCs and XP-A-iMCs.
(A) Schematic diagram of UV-B irradiation experiment with HC-iMCs and XP-A-iMCs. (B) The number of upregulated (magenta) and downregulated (green) probes at four or 12 h after low-dose (30 J/m^2) or high-dose (150 J/m^2) UV-B irradiation compared to pre-irradiation is indicated in the stacked bar graphs. When HC-iMCs were exposed to low-dose UV-B, the expression levels of 27 probes (15 upregulated and 12 downregulated) changed by > 10-fold 4 h after irradiation compared with pre-irradiation levels. Almost all genes returned to pre-irradiation levels 12 h after irradiation. Alternatively, when XP-A-iMCs were irradiated with low-dose UV-B, the expression levels of 72 probes (34 upregulated and 38 downregulated) substantially changed 4 h after irradiation. (C) Expression kinetics in each iMCs on the upregulated probes (n = 26, left panel) and the downregulated probes (n = 55, right panel) in HC-iMCs (> 10FC, 4 h after high-dose (150 J/m^2) UV-B irradiation).

pathophysiology of XP because freckle-like pigmented maculae are the most early and inevitably observed symptoms. XP-A-iMCs and HC-iMCs were successfully established. They are morphologically alike NHEMs and positive for MC markers (Fig. 2A-C) and melanin synthesis (Fig. 3C). The exact molecular mechanism underlying the clinical symptoms of XP has not yet been clarified [1,2]. Therefore, global gene expression patterns of XP-A-iMCs were investigated with the primary focus on the effect of UV-B irradiation on XP-A-iMCs.

Comparison of the basal gene expression levels (i.e., without UV-B irradiation) between XP-A-iMCs and HC-iMCs were conducted. We

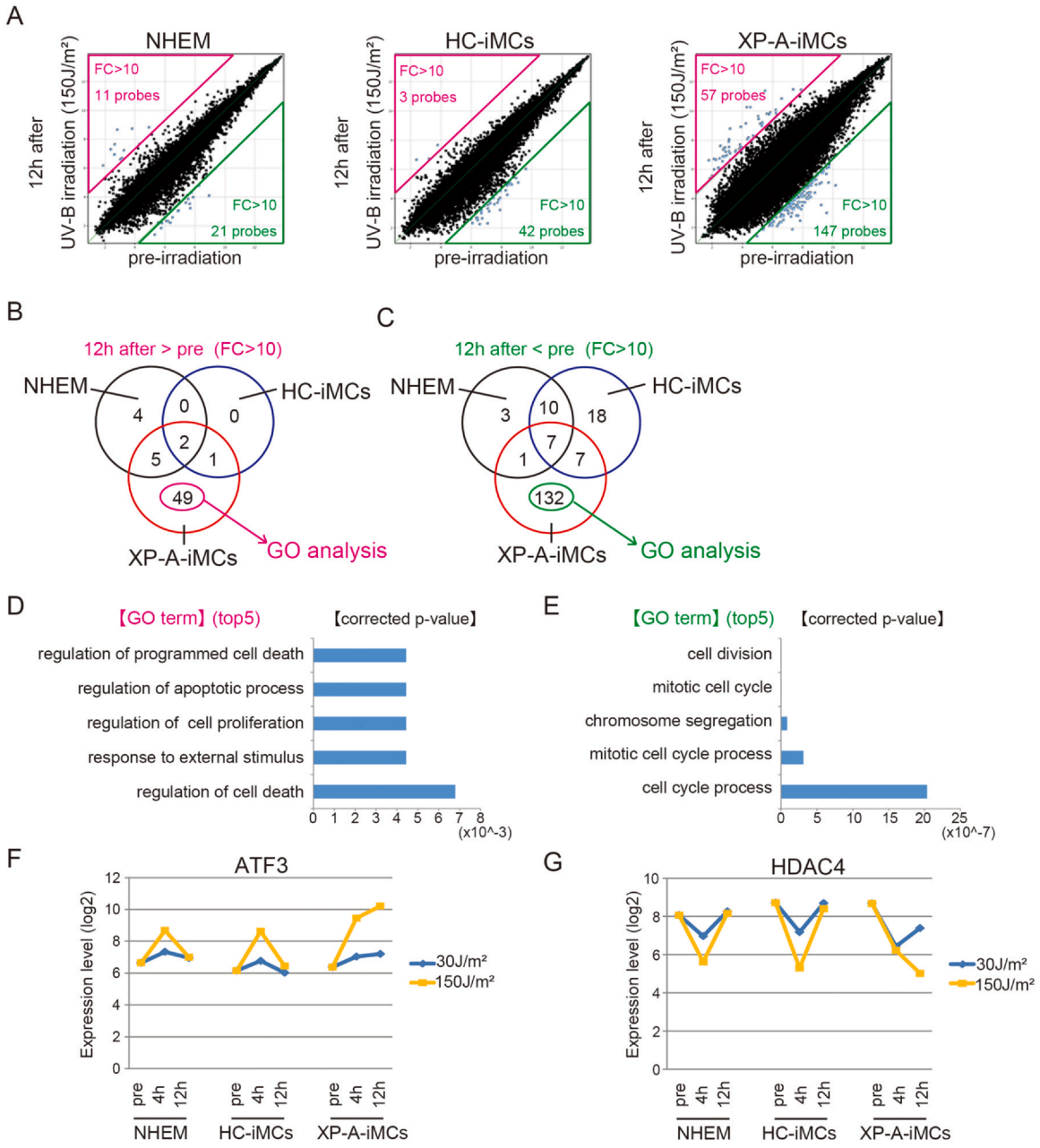

Fig. 5. Verification of molecular mechanisms in XP-A-iMCs when exposed to high-dose of UV-B.
(A) Comparison of global gene expression levels between the control (pre-irradiation, *x*-axis) and high-dose (150 J/m^2) UV-B-treated (12 h after irradiation, *y*-axis) NHEMs, HC-iMCs, and XP-A-iMCs. The numbers of upregulated (magenta) and downregulated (green) probes (> 10-fold differences) are indicated in each graph.(B)(C) Venn diagram indicating overlapping of upregulated (B) and downregulated (C) probes at 12 h after high-dose UV-B irradiation compared to pre-irradiation among the three cell types. Black, blue, and red circles refer to NHEMs, HC-iMCs, and XP-A-iMCs, respectively. (D) (E) The top five enriched GO terms of XP-A-iMC-specific upregulated genes (D) and XP-A-iMC-specific downregulated genes (E) arranged from top to bottom in ascending order of corrected *p*-values. (F) Changes in the expression levels of a representative XP-A-iMC-specific upregulated gene (*ATF3*) pre-irradiation and four and 12 h after UV-B treatment (30 or 150 J/m^2) are indicated. (G) Changes in the expression levels of a representative XP-A-iMC specific downregulated gene (HDAC4) pre-irradiation and four and 12 h after UV-B treatment (30 or 150 J/m^2) are indicated.

identified commonly upregulated (XP-A-iMCs > HC-iMCs) 7 genes and downregulated (XP-A-iMCs < HC-iMCs) 9 genes (Fig. 2D-2F). However, expressions pattern of these genes were not different between XP-A and healthy control fibroblasts. Among the downregulated genes in XP-A-iMCs, *CHCHD2*, which has been associated with Parkinson's disease, is reportedly a negative regulator of mitochondria-mediated apoptosis, while its loss-of function mutation causes upregulation of apoptotic signaling through mitochondrial dysfunction [19]. Mitochondrial dysfunction is a common characteristic in aging, which corresponds with that XP is an aging/photoaging model, and previous reports indicated XP-A cells showed defective mitophagy [20]. It also indicates the importance of selecting an appropriate cell type to investigate the disease pathophysiology.

This study is the first to demonstrate that the DNA repair level of XP-A MCs is reduced to a similar level to XP-A fibroblasts. It is reasonable to expect that XP-iMCs are incapable to repair DNA photolesions. Alternatively, MCs are resistant to UV-induced apoptosis [21]. Consequently, it was uncertain that the DNA repair ability of XP-iMCs was impaired, until we obtained the present results (Fig. 3A).

Expression profile analysis of XP-A-iMCs exposed to UV-B was used to gain insights into the clinical symptoms of XP. Global gene

expression analysis was conducted under the condition that MCs are vital and not in a state of function loss, including melanogenesis (Fig. S4). Melanin content was chemically determined before and 24 h after UV-B irradiation (Fig. 3C). Melanin content were varied among cell strains, possibly due to the skin color of the donor [13]. But it was not significantly changed after UV irradiation in the present experimental conditions, which goes along with expression profile data of TYR, SOX10, and MITF (Fig. S4). In the comparison of gene expression profile between XP-A-iMCs and HC-iMCs after irradiation with the same doses, the most noticeable finding was that numerous gene probes that were specifically upregulated/downregulated in XP-A-iMCs after high-dose (150 J/m^2) UV-B irradiation did not return to basal levels. These results seem to be quite natural since, at the same dose, much more DNA photolesions remains in XP-A-MCs than HC-iMCs, and genes that respond to DNA photolesions need more time to return to basal levels, implying that specific characteristics might be correlated with the clinical features of XP-A (Fig. 4C).

Functional analysis with NHEMs as reference identified 49 and 132 probes in XP-A-iMCs that were specifically upregulated and downregulated, respectively, 12 h after high-dose UV-B irradiation (Fig. 5B, Table S1 and S2). Among specifically upregulated 49 genes in XP-A-iMCs (Fig. 5A, B, and Table S1), *ATF3* is known to be involved in transcription of regulating apoptosis via stress response. ATF3 was also identified among p53-target genes induced in normal MCs in response to UV-B exposure [22]. Since TP53 is expressed in response to DNA lesions, it is reasonable that XP-A-iMCs express much higher levels of p53-target genes due to NER deficiency. Among 132 genes specifically downregulated in XP-A-iMCs, *BUB1*, *BUB1B*, *CDC20* and *TOP2A* are functional in cell cycle regulation. UV-induced inhibition of *HDAC4* reportedly increases MMP1 in normal human melanocytes and have been implicated in photoaging [23], In the present study we showed continual downregulation of HDAC4 upon UV exposure and specifically upregulation of MMP1 even low dose UV exposure in XP-A-iMCs (Fig. 5G, and Table S2, S5). It partly explains the pathophysiology of accelerated photoaging in XP-A.

Regarding comparison between expression profiles in response to similar biological insults for XP-A-iMCs and HC-iMCs, namely UV-B irradiation with 30 and 150 J/m^2, respectively, to achieve the same surviving fraction of 10 % using the colony formation assay, the expression of 14 gene probes was upregulated > 10-fold in XP-A-iMCs exposed to 30 J/m^2, in comparison to HC-iMCs exposed to 150-J/m^2 (Fig. S4, Table S5, S6). GO analysis showed that the most highly upregulated gene pathways were “cytokine activity” and “cytokine receptor binding,” which agree with the previously reported findings that skin cells of *Xpa*-knockout mice showed specific upregulation of genes in inflammatory response pathways [24]. These facts partly explain the characteristic clinical features of XP-A, such as extreme sunburn in response to a minimum sunlight exposure that can persist for more than 96 h (Fig. 4C) [2].

In conclusion, MCs were successfully established from XP-A-iPSCs and exhibited similar reductions in DNA repairability as XP-A fibroblasts. Expression array analysis demonstrated remarkable differences in the gene expression profiles of XP-A-iMCs and HC-iMCs at the basal level, whereas an insignificant difference between XP-A and HC fibroblasts, indicating the importance of selecting the appropriate target cells.

In XP-A MCs, apoptotic pathways were highly upregulated at the same high-dose UV exposure as HC-iMCs, and ‘cytokine-related pathways’ were specifically upregulated even at low-dose UV exposure, this explains some of the clinical features of XP-A. This work clarified the usefulness of disease-specific iPS cells and the importance of selecting appropriate target cells. The plan was to employ this technique for developing treatment strategies for intractable diseases.

Funding sources

This research was supported by the Japan Agency for Medical Research and Development (AMED) under Grant Numbers JP15ek0109028 (CN, MK, TA), JP20ek0109450 (CN, MK), JP16bm0704005 (TA), JP23ym0126809 (TF), and JP24ym0126809 (TF), JSPS KAKENHI Grant Number JP16K10156 (CN), Japan Ministry of the Health, Labor and Welfare; Grant Number 20FC1043 (CN), research assistance funds from Shinryokukai General Incorporated Association (TA), Akira Sakagami Fund for Research and Education, Kobe University Graduate School of Medicine (M K-A and TA), KOSÉ Cosmetology Research Foundation (TF), Kinoshita memorial enterprise subsidy (TF), The POLA R&M Grant for Vitiligo Research (TF), Atsushi Kukita Award from the Japanese Society of Pigment Cell Research (TF), The Naito Foundation (TF), and the Ichiro Kanehara Foundation (TF).

CRediT authorship contribution statement

Chihiro Takemori: Methodology, Investigation, Writing and Editing, Visualization, Validation, **Michiyo Koyanagi-Aoi:** Methodology, Investigation, Software, Data curation, Writing and Editing, Visualization, Validation, **Takeshi Fukumoto:** Methodology, Investigation, Writing and Editing, Visualization, **Kazumasa Wakamatsu:** Melanin quantification and its interpretation, writing and editing, **Shosuke Ito:** Melanin quantification and its interpretation, Writing and Editing, **Makoto Kunisada:** Investigation, Writing and Editing, **Chieko Hosaka:** Writing and Editing, **Seiji Takeuchi:** Writing and Editing, **Akiharu Kubo:** Writing and Editing, **Takashi Aoi:** Conceptualization, Writing and Editing, Validation, Supervision, **Chikako Nishigori:** Conceptualization, Methodology, Investigation, Writing and Editing, Validation, Supervision

Declaration of Competing Interest

The authors declare no conflicts of interest.

Acknowledgements

We thank Mari Kohmoto for technical advice and support.

Appendix A. Supporting information

Supplementary data associated with this article can be found in the online version at doi:10.1016/j.jdermsci.2024.06.004.

References

[1] J.E. Cleaver, Defective repair replication of DNA in xeroderma pigmentosum, Nature 218 (1968) 652–656.
[2] C. Nishigori, E. Nakano, T. Masaki, R. Ono, S. Takeuchi, M. Tsujimoto, et al., Characteristics of xeroderma pigmentosum in japan: lessons from two clinical surveys and measures for patient care, Photochem. Photobiol. 95 (1) (2019) 140–153.
[3] I. Satokata, K. Tanaka, N. Miura, I. Miyamoto, Y. Satoh, S. Kondo, et al., Characterization of a splicing mutation in group A xeroderma pigmentosum, Proc. Natl. Acad. Sci. USA 87 (1990) 9908–9912.
[4] K. Imoto, C. Nadem, S. Moriwaki, C. Nishigori, K.-S. Oh, S.G. Khan, et al., Ancient origin of a Japanese xeroderma pigmentosum founder mutation, J. Dermatol. Sci. 69 (2) (2013) 175–176.
[5] K. Takahashi, K. Tanabe, M. Ohnuki, M. Narita, T. Ichisaka, K. Tomoda, et al., Induction of pluripotent stem cells from adult human fibroblasts by defined factors, Cell 131 (5) (2007) 861–872.
[6] K. Okamura, H. Sakaguchi, R. Sakamoto-Abutani, M. Nakanishi, K. Nishimura, M. Yamazaki-Inoue, et al., Distinctive features of single nucleotide alterations in induced pluripotent stem cells with different types of DNA repair deficiency disorders, Sci. Rep. 6 (2016) 26342.
[7] L. Fu, X. Xu, R. Ren, J. Wu, W. Zhang, J. Yang, et al., Modeling xeroderma pigmentosum associated neurological pathologies with patients-derived iPSCs, Protein Cell 7 (3) (2016) 210–221.

[8] C. Hosaka, M. Kunisada, M. Koyanagi-Aoi, T. Masaki, C. Takemori, M. Taniguchi-Ikeda, et al., Induced pluripotent stem cell-derived melanocyte precursor cells undergoing differentiation into melanocytes, Pigment Cell Melanoma Res. 32 (5) (2019) 623–633.
[9] E. Nakano, S. Takeuchi, R. Ono, M. Tsujimoto, T. Masaki, C. Nishigori, Xeroderma pigmentosum diagnosis using a flow cytometry-based nucleotide excision repair assay, J. Invest. Dermatol. 138 (2) (2018) 467–470.
[10] T. Matsunaga, K. Hieda, O. Nikaido, Wavelength dependent formation of thymine dimers and (6-4) photoproducts in DNA by monochromatic ultraviolet light ranging from 150 to 365 nm, Photochem. Photobiol. 54 (3) (1991) 403–410.
[11] S. Ito, Y. Nakanishi, R.K. Valenzuela, M.H. Brilliant, L. Kolbe, K. Wakamatsu, Usefulness of alkaline hydrogen peroxide oxidation to analyze eumelannin and pheomelanin in various tissue samples: applicattion to chemical analysis of human hair melanins, Pigment Cell Melanoma Res. 24 (4) (2011) 605–613.
[12] K. Wakamatsu, S. Ito, J.L. Rees, The usefulness of 4-amino-3-hydroxyphenylalanine as a specific marker of pheomelanin, Pigment Cell Res. 15 (3) (2002) 225–232.
[13] S. Del Bino, S. Ito, J. Sok, Y. Nakanishi, P. Bastien, K. Wakamatsu, et al., Chemical analysis of constitutive pigmentation of human epidermis reveals constant eumelanin to pheomelanin ratio, Pigment Cell Melanoma Res. 28 (6) (2015) 707–717.
[14] S. Takeuchi, T. Fukumoto, C. Takemori, N. Saito, C. Nishigori, M. Sato, Cell migration is impaired in XPA-deficient cells, FASEB Bioadv 5 (2) (2022) 53–61.
[15] Y. Auclair, R. Rouget, E.B. Affar, E.A. Drobetsky, ATR kinase is required for global genomic nucleotide excision repair exclusively during S phase in human cells, Proc. Natl. Acad. Sci. USA 105 (46) (2008) 17896–17901.
[16] F. Bélanger, V. Rajotte, E.A. Drobetsky, A majority of human melanoma cell lines exhibits an S phase-specific defect in excision of UV-induced DNA photoproducts, PLoS One 9 (1) (2014) e85294.
[17] S. Gaddameedhi, M.G. Kemp, J.T. Reardon, J.M. Shields, S.L. Smith-Roe, W.K. Kaufmann, et al., Similar nucleotide excision repair capacity in melanocytes and melanoma cells, Cancer Res. 70 (12) (2010) 4922–4930.
[18] A. Shinya, C. Nishigori, S. Moriwaki, H. Takebe, M. Kubota, A. Ogino, et al., A case of Rothmund-Thomson syndrome with reduced DNA repair capacity, Arch. Dermatol. 129 (3) (1993) 332–336.
[19] H. Meng, C. Yamashita, K. Shiba-Fukushima, T. Inoshita, M. Funayama, S. Sato, et al., Loss of Parkinson's disease-associated protein CHCHD2 affects mitochondrial crista structure and destabilizes cytochrome c, Nat. Commun. 8 (2017) 15500.
[20] E.F. Fang, M. Scheibye-Knudsen, L.E. Brace, H. Kassahun, T. SenGupta, H. Nilsen, et al., Defective mitophagy in XPA via PARP-1 hyperactivation and NAD(+)/SIRT1 reduction, Cell 157 (4) (2014) 882–896.
[21] T. Fukumoto, T. Iwasaki, T. Okada, T. Hashimoto, Y. Moon, M. Sakaguchi, et al., High expression of Mcl-1L via the MEK-ERK-phospho-STAT3 (Ser727) pathway protects melanocytes and melanoma from UVB-induced apoptosis, Genes Cells, 21 (2) (2016) 185–199.
[22] G. Yang, G. Zhang, M.R. Pittelkow, M. Ramoni, H. Tsao, Expression profiling of UVB response in melanocytes identifies a set of p53-target genes, J. Invest. Dermatol. 126 (11) (2006) 2490–2506.
[23] Y. Lee, M.H. Shin, M.-K. Kim, C.-H. Park, H.S. Shin, D.H. Lee, et al., Ultraviolet irradiation-induced inhibition of histone deacetylase 4 increases the expression of matrix metalloproteinase-1 but decreases that of type I procollagen via activating JNK in human dermal fibroblasts, J. Dermatol. Sci. 101 (2) (2021) 107–114.
[24] M. Kunisada, C. Hosaka, C. Takemori, E. Nakano, C. Nishigori, CXCL1 Inhibition regulates UVB-induced skin inflammation and tumorigenesis in Xpa-deficient mice, J. Invest. Dermatol. 137 (9) (2017) 1975–1983.